Brain areas with normatively greater cerebral perfusion in early life may be more susceptible to beta amyloid deposition in late life

Irene B. Meier [a,b,*], Patrick J. Lao [b], Anton Gietl [a], Robert S. Vorburger [b], José Gutierrez [c], Christopher M. Holland [d], Charles R.G. Guttmann [e], Dominik S. Meier [e], Alfred Buck [f], Roger M. Nitsch [a,g], Christoph Hock [a,g], Paul G. Unschuld [a], Adam M. Brickman [b,c]

[a] Institute for Regenerative Medicine IREM, University of Zurich, 8952 Zurich, Switzerland
[b] Taub Institute for Research on Alzheimer's Disease and the Aging Brain, College of Physicians and Surgeons, Columbia University, New York, NY 10032, USA
[c] Department of Neurology, College of Physicians and Surgeons, Columbia University, New York, NY 10032, USA
[d] Carolina Neurosurgery & Spine Associates, Charlotte, NC 28204, USA
[e] Center for Neurological Imaging, Brigham and Women's Hospital, Harvard Medical School, Boston MA 02215, USA
[f] University Hospital Zurich, Clinic for Nuclear Medicine, Zurich, 8091, Switzerland
[g] Neurimmune, Schlieren, Switzerland

ARTICLE INFO

ABSTRACT

Background: The amyloid cascade hypothesis characterizes the stereotyped progression of pathological changes in Alzheimer's disease (AD) beginning with beta amyloid deposition, but does not address the reasons for amyloid deposition. Brain areas with relatively higher neuronal activity, metabolic demand, and production of reactive oxygen species in earlier life may have higher beta amyloid deposition in later life. The aim of this study was to investigate early life patterns of perfusion and late life patterns of amyloid deposition to determine the extent to which normative cerebral perfusion predisposes specific regions to future beta amyloid deposition.

Materials and Methods: One hundred twenty-eight healthy, older human subjects (age: 56–87 years old; 44% women) underwent positron emission tomography (PET) imaging with [^{11}C]PiB for measures of amyloid burden. Cerebral perfusion maps derived from 47 healthy younger adults (age: 22–49; 47%) who had undergone single photon emission computed tomography (SPECT) imaging, were averaged to create a normative template, representative of young, healthy adults. Perfusion and amyloid measures were investigated in 31 cortical regions from the Hammers atlas. We examined the spatial relationship between normative perfusion patterns and amyloid pathophysiology.

Results: The pattern of increasing perfusion (temporal lobe<parietal lobe<frontal lobe<insula/cingulate gyrus<occipital lobe; F(4,26)=7.8, *p* = 0.0003) in young, healthy adults was not exactly identical to but approximated the pattern of increasing amyloid burden (temporal lobe<occipital lobe<frontal lobe<parietal lobe<insula/cingulate gyrus; F(4,26)=5.0, *p* = 0.004) in older adults. However, investigating subregions within cortical lobes provided consistent agreement between ranked normative perfusion patterns and expected Thal staging of amyloid progression in AD (Spearman *r* = 0.39, *p* = 0.03).

Conclusion: Our findings suggest that brain areas with normatively greater perfusion may be more susceptible to amyloid deposition in later life, possibly due to higher metabolic demand, and associated levels of oxidative stress and inflammation.

1. Introduction

The deposition of cerebral amyloid-β throughout the cortical mantle is a hallmark of Alzheimer's disease (AD). Amyloid pathology is not distributed uniformly [1], and recent studies have turned to the examination of perfusion and metabolic patterns in the aging brain to help

explain this regional variability [2,3]. The pattern of amyloid deposition is associated with diminished regional cerebral blood flow (CBF) cross-sectionally [4]. In animal models, mild chronic cerebral hypoperfusion can create a metabolically deregulated microenvironment that triggers entry and accumulation of peripherally applied amyloid peptides [5]. On the other hand, amyloid deposition in brain arteries may induce

hypoperfusion via decreases in vasodilation [6] or impaired clearance of pathology [7], and lead to subsequent neurological deficits [8]. Thus, it is likely that there is a positive feedback loop in which vascular perturbations potentiate amyloid pathology, which, in turn, decreases vascular function and affect metabolic processes.

The association between amyloid and perfusion or metabolism can be thought of as biphasic over the life course in which there is a positive association prior to downstream damage from amyloid accumulation followed by a negative association after downstream damage has occurred [9]. There is some evidence that amyloid deposition occurs in areas of higher metabolism and activity [10]. Neuronal activity regulates amyloid precursor protein (APP) processing in the mammalian brain [11], and brain regions in healthy adults with higher neural activity are also the regions to accumulate amyloid in AD [9]. Similarly, brain regions with higher metabolic demand may promote amyloid deposition via chronic oxidative stress and associated inflammatory changes [12]. However, among symptomatic individuals, areas of high amyloid burden are associated with lower neuronal activity and metabolism [9,13].

The extent to which regional blood perfusion patterns over long periods of time affect AD pathology deposition is less clear. In humans, long-term longitudinal studies (i.e., over decades) that examine patterns of cerebral perfusion and amyloid deposition are logistically difficult. To circumvent this issue, we examined the spatial distribution of fibrillar amyloid deposition in older adults as a function of normative cerebral perfusion values derived from younger, healthy adults. We tested whether increased amyloid is disproportionately present in areas that show normatively decreased or increased cerebral perfusion.

2. Materials and methods

2.1. Participants

One hundred twenty-eight older adults (mean age$\pm$SD=69.7 $\pm$ 6.2 years, 44% women) [13] underwent detailed screening as well as neurological and neuropsychological evaluation. While 24% of subjects were classified as amyloid positive, amyloid uptake was considered a continuous variable due to its distribution of uptake values. Only individuals without dementia and depression, defined by the Mini-Mental State Examination (scores$\geq$27) for healthy controls, and according to standard criteria for MCI [34] after a comprehensive clinical and neuropsychological workup, and the Hamilton Depression Rating Scale [14] (17 item, score $\leq$12) were included. Exclusion criteria included neurologic, psychiatric, or major medical illness, medication, or history of drug abuse that might affect cognition, as previously described [13]. Twenty-one percent of participants had mild cognitive impairment, and the remaining were cognitively unimpaired. This research was approved the cantonal ethics committee Zurich and informed consent was obtained from all participants.

2.2. PiB PET imaging

Amyloid PET scans (intravenous administration of 350 MBq [^{11}C]PiB, GE Discovery PET/CT scanner) were performed in the Division of Nuclear Medicine, Zurich University Hospital [15]. A maximum probability atlas was used to define regions of interest (ROIs) based on gray and white matter segmentation of each subject's structural MRI scan. PET images were co-registered with the subject's T1-weighted MRI scan. Standard uptake value ratios (SUVRs) were calculated with PET data 50–70 min post-injection and a cerebellar reference region [13]. Subjects' T1-weighted MRI scans were spatially normalized to perform all further analyses in Montreal Neurological Institute (MNI) space [16]. Mean PiB SUVRs were calculated for 5 cortical lobes and 31 cortical subregions defined by the Hammers Atlas [17], averaging across hemispheres and across all subjects.

2.3. SPECT imaging and normative blood perfusion atlas

Single photon emission computed tomography (SPECT; intravenous administration of 1000 MBq [^{99m}Tc]ethylene cysteinate, Picker Prism 3000 gamma camera) images from 47 young, healthy adults (mean age$\pm$SD=34.3 $\pm$ 7.6 yrs, 47% women; data from the Society of Nuclear Medicine Brain Imaging Council) were obtained for the creation of a normative cerebral perfusion template [18]. Briefly, raw SPECT images were low-pass filtered (order=4.0, cutoff=0.26) and proportionally scaled to 0 to 1000 relative perfusion units. The normative perfusion template was created by averaging each subject's relative perfusion image in MNI space. Mean cerebral perfusion was calculated in the same 5 cortical lobes and 31 cortical subregions of the Hammers atlas that were used to derive PiB SUVR values for direct comparison between modalities and groups.

2.4. Statistical analyses

Univariate analysis of variance (ANOVA) was used to determine whether mean PiB SUVR differed across the 5 cortical lobes defined by the Hammers atlas. We tested the omnibus effect and the mean differences across ROIs. Test statistics, degrees of freedom, and exact p-values are shown for the omnibus effect, and 95% confidence intervals and their associated p-values are shown for pair-wise comparisons (Table 1). A Spearman correlation was used to test the association between ranked normative perfusion values and ranked mean PiB SUVR where each data point represents a cortical subregion. The Spearman correlation accounts for the non-independence of nearby subregions (e.g., within the same lobe).

3. Theory

Although it is unclear how blood perfusion patterns over time affect AD and the underlying mechanisms that link cerebral perfusion to amyloid deposition are unknown, elevated synaptic activity increases amyloid levels in the interstitial fluid of the brain and increases vesicle exocytosis, providing further evidence that metabolism may modulate region-specific amyloid deposition [19]. In transgenic AD mouse models, endogenous neuronal activity regulates the regional concentration of amyloid in the interstitial fluid, which drives local amyloid aggregation [19]. Compared with previous findings that focused on metabolism [30], cerebral perfusion levels capture additional mechanical and physical factors such as blood pressure, vasodilation/constriction, blood viscosity and hemodynamics that could lead to regional vulnerability for pathology over long periods of time.

There has been increasing attention placed on cerebrovascular contributions to cognitive decline, especially given the high prevalence of dementia due to multiple etiologies [20–22]. The association between cerebral perfusion and cognition has been investigated as a function of amyloid burden in the Alzheimer's Disease Neuroimaging Initiative (ADNI) study, where higher CBF in hippocampus, posterior cingulate, and precuneus was associated with poorer memory performance in amyloid positive individuals [23]. Studies also report a positive correlation between CBF and amyloid burden in the hippocampus, amygdala, and caudate, frontal, temporal, and insula of healthy individuals with high levels of amyloid versus low amyloid burden, suggesting a compensatory hemodynamic mechanism aimed at maintaining stable blood perfusion and oxygen supply, and at protecting against pathology in early stages of AD [24]. Furthermore, lower cerebral perfusion in symptomatic individuals compared to non-symptomatic individuals in the precuneus, entorhinal cortex, hippocampus, parietal cortex, and temporal cortex has been reported [25,26]. Therefore, the association between higher cerebral perfusion and higher amyloid burden may be a transient event that surges before clinical disease onset and reverses as AD progresses, when downstream damage from amyloid may impair cerebrovascular function.

Table 1

Posthoc pairwise comparisons of Normative Perfusion (above diagonal) and PiB SUVR (below diagonal) by Cortical Lobe.

	Occipital Lobe	Insula/ Cingulate Gyrus	Frontal Lobe	Parietal Lobe	Temporal Lobe
Mean difference (Row – Column) [95% confidence interval]					
Exact p-value					
Occipital Lobe	n/a	51 [-34, 136] p=0.23	113 [46, 180] p=0.002	124 [39, 209] p=0.006	168 [100, 237] p<0.001
Insula/ Cingulate Gyrus	0.15 [0.02, 0.28] p=0.03	n/a	62 [-5, 129] p=0.07	73 [-12. 158] p=0.09	117 [49, 186] p=0.002
Frontal Lobe	0.06 [-0.04, 0.16] p=0.24	-0.09 [-0.19, 0.01] p=0.09	n/a	11 [-56, 78] p=0.74	55 [10, 100] p=0.02
Parietal Lobe	0.08 [-0.05, 0.21] p=0.24	-0.07 [-0.20, 0.06] p=0.25	0.02 [-0.09, 0.12] p=0.77	n/a	44 [-24, 112] p=0.20
Temporal Lobe	-0.04 [-0.15, 0.06] p=0.39	-0.19 [-0.30, -0.09] p=0.001	-0.11 [-0.17, -0.04] p=0.004	-0.12 [-0.23, -0.02] p=0.03	n/a

Table 2

Rank Order of Normative Perfusion Values.

| Ranked Normative Perfusion	ROI	Ranked Normative Perfusion	ROI
1	Lateral anterior temporal lobe	16	Middle frontal gyrus
2	Medial anterior temporal lobe	17	Lateral occipital lobe
3	Lateral orbital gyrus	18	Subgenual frontal cortex
4	Anterior orbital gyrus	19	Posterior orbital gyrus
5	Parahippocampal and ambient gyri	20	Superior frontal gyrus
6	Fusiform gyrus	21	Superior parietal gyrus
7	Hippocampus	22	Anterior cingulate gyrus
8	Anterior superior temporal gyrus	23	Inferior frontal gyrus
9	Amygdala	24	Straight gyrus
10	Inferiolateral parietal lobe	25	Subcallosal area
11	Middle and inferior temporal gyrus	26	Posterior superior temporal gyrus
12	Medial orbital gyrus	27	Pre-subgenual frontal cortex
13	Postcentral gyrus	28	Posterior cingulate gyrus
14	Posterior temporal lobe	29	Insula
15	Precentral gyrus	30	Lingual gyrus
		31	Cuneus

4. Results

Normative perfusion differed by cortical lobe (F(4,26)=7.8, p = 0.0003), and the general trend in normative perfusion was as follows: temporal lobe<parietal lobe<frontal lobe<insula/cingulate gyrus<occipital lobe (Fig. 1). Amyloid burden also differed by cortical lobe (F(4,26)=5.0, p = 0.004), and the general trend was temporal lobe<occipital lobe<frontal lobe<parietal lobe<insula/cingulate gyrus (Fig. 1). Post-hoc pairwise comparisons of normative perfusion and mean PiB SUVR between cortical lobes are listed in Table 1. Biomarker values of subregions are displayed as points within the boxplot for each lobe (Fig. 1), each dot representing one subregion of the respective lobe.

Table 2 shows the ranked normative perfusion of subregions within cortical lobes. Fig. 2 demonstrates the posterior to anterior gradient of high to low normative perfusion values. Taken together, Table 2 and Fig. 2 demonstrate that normative perfusion was not uniform within cortical lobes. Areas with high amyloid burden and high normative perfusion included posterior cingulate gyrus, insula, cuneus, lingual gyrus, and pre-subgenual anterior cingulate. Areas that had low amyloid burden and low normative perfusion values included parahippocampal and ambient gyri, orbito-frontal cortex anterior orbital gyrus, orbito-frontal cortex lateral orbital gyrus, anterior temporal lobe medial, and anterior temporal lobe (inferior and lateral). Fig. 3 shows the positive Spearman correlation between ranked normative perfusion and ranked mean PiB SUVR for subregions (r = 0.39, p = 0.03).

5. Discussion

The observed distribution of amyloid in the older participants included in this study was similar to previously described patterns of amyloid PET [27–29] and amyloid pathology [1]. The pattern of increasing normative perfusion in cortical lobes (temporal lobe<parietal lobe<frontal lobe<insula/cingulate gyrus<occipital lobe) was not entirely congruent with the pattern of increasing amyloid burden (temporal lobe<occipital lobe<frontal lobe<parietal lobe<insula/cingulate gyrus) in older adults. The discrepancy between normative perfusion, which are heterogeneous across cortical lobes, and amyloid deposition, which are homogeneous across cortical lobes, suggest that increased

Normative Perfusion by Cortical Lobe
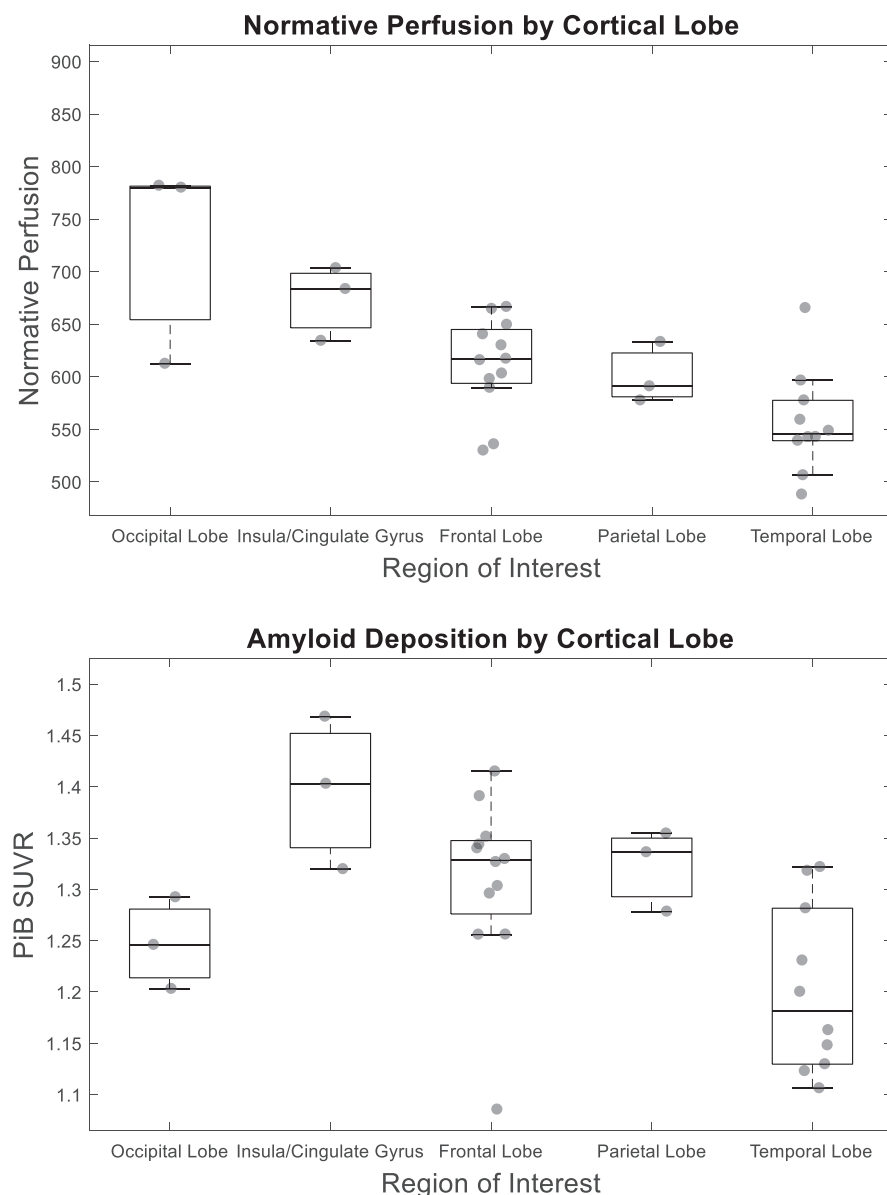
Fig. 1. Boxplots of Normative Perfusion and Mean PiB SUVR by Cortical Lobe.

Amyloid Deposition by Cortical Lobe

cerebral perfusion may be one out of many factors that promote amyloid deposition.

The findings of a spatial relationship between perfusion patterns in healthy, young adults and amyloid deposition in late life are consistent with the hypothesis that high metabolic demands throughout life promote AD pathology [30]. The distribution of aerobic glycolysis, the metabolic pathway of converting glucose into pyruvate, in normal young adults is spatially and positively correlated with amyloid deposition in AD patients and healthy older adult controls with elevated amyloid [30]. As cerebral glucose metabolism and cerebral perfusion are tightly linked, and to an extent, proxies of each other [31], our findings add to a growing body of work that implicates increased metabolism in early life to the development of AD pathology in later life [9,30]. Glucose and oxygen are necessary for neuronal function and are delivered to neurons via astrocytes. Astrocytes also regulate vasodilation and hence, local blood flow [32], which could contribute to our observation. An observation in mice by Hawkes et al. (2013) suggests that the regional differences in deposition of amyloid may be due to changing perivascular drainage of solutes and variations in vascular basement membrane with age, showing a thickening of capillary basement membrane in the

cerebral cortex, hippocampus, and the thalamus, but not in the striatum. It has also been proposed that amyloid-vulnerable brain regions are characterized by relatively low expression levels of gene sets involved protein synthesis and mitochondrial respiration [33], adding further evidence to the complexity of the pathophysiological mechanisms of AD and their impact on metabolism across the entire lifespan.

The comparison of two independent samples rather than a within-subject design (i.e., comparing perfusion and amyloid levels within the same participants at the same point in time) enabled us to establish normative perfusion/metabolic patterns to determine whether pathology differs as a function of this inter-regional variability, and to infer whether perfusion patterns may precipitate amyloid pathology. Of course, long-term longitudinal studies, in which cerebral perfusion is measured at very young age and then participants are followed over decades, would be required to confirm our findings. For a longitudinal study, it would be necessary to measure cerebral perfusion in those who will eventually develop substantial amyloid pathology, prior to the presence of amyloid pathology.

While future studies will be necessary to determine the differential impact of factors and biomarkers associated with the aging brain, our
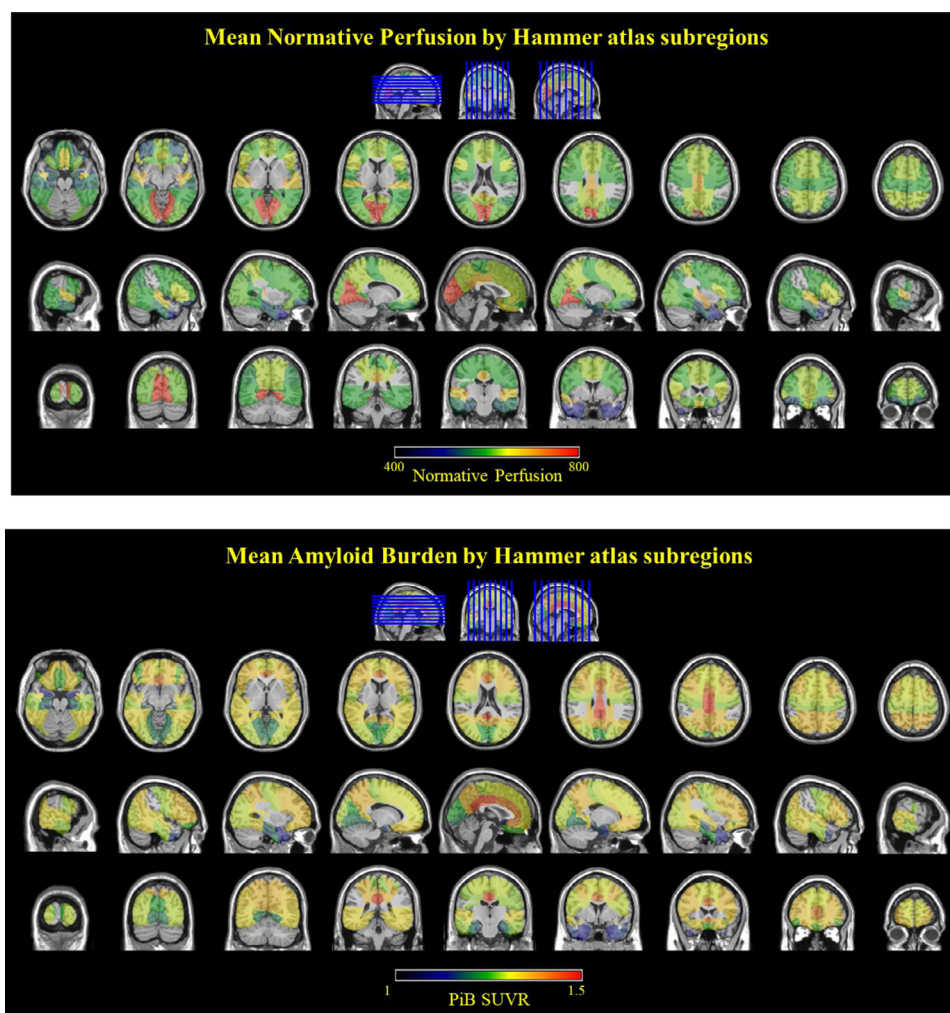
Fig. 2. Mean normative blood perfusion and amyloid burden in all subregions of cortical lobes.
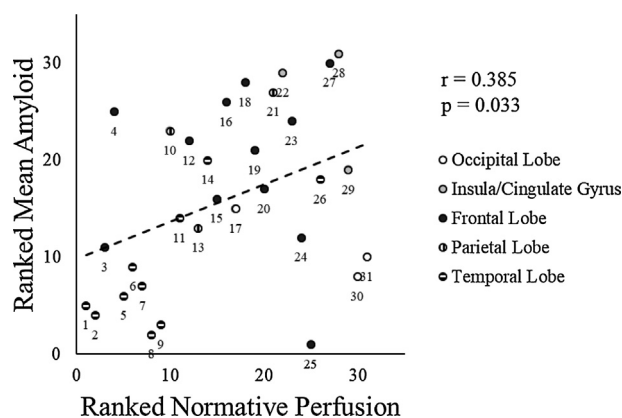

Fig. 3. Spearman correlation between ranked SPECT and ranked PiB SUVR across subregions. Mean regional PiB SUVR value in each region of interest (ROI) of blood perfusion appreciated through SPECT.

may have contributed to the underestimaion of mean perfusion values in regions defined by the Hammer atlas. The different amounts of white matter in each Hammer atlas region may be have contributed to regional differences (e.g., medial occipital lobe has little white matter and higher perfusion compared to lateral occipital lobe). The partial volume effects introduced by the inclusion of white matter and the different spatial resolution of the imaging modalities potentially introduced bias that was attenuated by spatially averaging across cortical lobes. Although we observed a spatial correlation between perfusion in the normative atlas and amyloid deposition in older participants, the effect sizes were modest. These findings are consistent with the hypothesis that the regionality of amyloid pathology in older adults may be partially due to normative perfusion patterns but highlight that there are likely many other contributing factors. However, the novelty of this study lies in its design, allowing the disassociation of regional early-life metabolic patterns from late-life pathology and hence raises the possibility that vascular factors prior to amyloid deposition, such as increased cerebral blood perfusion, could promote AD pathogenesis.

6. Conclusions

Our findings that there is a spatial overlap between early life perfusion and late life amyloid burden suggest that the regional distribution of amyloid deposition may be a consequence of differential cerebral perfusion patterns, such that areas with normatively greater perfusion in early life are potentially more susceptible to amyloid deposition in late life due to increased metabolic demand.

study highlights the relevance of lifelong processes that may potentially differentiate between healthy versus pathological aging. Limitations of the study include the lack of access to data on APOE4 status of subjects, the inclusion of differing amounts of white matter in Hammer atlas subregions, and the different spatial resolution of PET and SPECT. Given the available data, we were unable to restrict perfusion values to gray matter. Therefore, the contribution of low perfusion in white matter

Declaration of Competing Interest

Nothing to report.

Acknowledgements

References

[1] D.R. Thal, et al., Phases of A beta-deposition in the human brain and its relevance for the development of AD, Neurology 58 (12) (2002) 1791–1800.

[2] R.L. Buckner, et al., Molecular, structural, and functional characterization of Alzheimer's disease: evidence for a relationship between default activity, amyloid, and memory, J. Neurosci. 25 (34) (2005) 7709–7717.

[3] A.D. Cohen, et al., Basal cerebral metabolism may modulate the cognitive effects of Abeta in mild cognitive impairment: an example of brain reserve, J. Neurosci. 29 (47) (2009) 14770–14778.

[4] Z. Cselenyi, L. Farde, Quantification of blood flow-dependent component in estimates of beta-amyloid load obtained using quasi-steady-state standardized uptake value ratio, J. Cereb. Blood Flow Metab. 35 (9) (2015) 1485–1493.

[5] A. ElAli, et al., Mild chronic cerebral hypoperfusion induces neurovascular dysfunction, triggering peripheral beta-amyloid brain entry and aggregation, Acta Neuropathol. Commun. 1 (2013) 75.

[6] J.M. Price, et al., Physiological levels of beta-amyloid induce cerebral vessel dysfunction and reduce endothelial nitric oxide production, Neurol. Res. 23 (5) (2001) 506–512.

[7] B.V. Zlokovic, The blood-brain barrier in health and chronic neurodegenerative disorders, Neuron 57 (2) (2008) 178–201.

[8] F.L. Princz-Kranz, et al., Vascular response to acetazolamide decreases as a function of age in the arcA beta mouse model of cerebral amyloidosis, Neurobiol. Dis. 40 (1) (2010) 284–292.

[9] W.J. Jagust, E.C. Mormino, Lifespan brain activity, beta-amyloid, and Alzheimer's disease, Trends Cognit. Sci. 15 (11) (2011) 520–526.

[10] R.L. Buckner, et al., Cortical hubs revealed by intrinsic functional connectivity: mapping, assessment of stability, and relation to Alzheimer's disease, J. Neurosci. 29 (6) (2009) 1860–1873.

[11] R.M. Nitsch, et al., Release of amyloid beta-protein precursor derivatives by electrical depolarization of rat hippocampal slices, Proc. Natl. Acad. Sci. USA 90 (11) (1993) 5191–5193.

[12] M.F. Beal, Aging, energy, and oxidative stress in neurodegenerative diseases, Ann. Neurol. 38 (3) (1995) 357–366.

[13] A.F. Gietl, et al., Regional cerebral blood flow estimated by early PiB uptake is reduced in mild cognitive impairment and associated with age in an amyloid-dependent manner, Neurobiol. Aging 36 (4) (2015) 1619–1628.

[14] M. Hamilton, A rating scale for depression, J. Neurol. Neurosurg. Psychiatry 23 (1960) 56–62.

[15] S.C. Steininger, et al., Cortical amyloid beta in cognitively normal elderly adults is associated with decreased network efficiency within the cerebro-cerebellar system, Front. Aging Neurosci. 6 (2014) 52.

[16] A.C. Evans, et al., Anatomical mapping of functional activation in stereotactic coordinate space, Neuroimage 1 (1) (1992) 43–53.

[17] A. Hammers, et al., Three-dimensional maximum probability atlas of the human brain, with particular reference to the temporal lobe, Hum. Brain Mapp. 19 (4) (2003) 224–247.

[18] C.M. Holland, et al., Spatial distribution of white-matter hyperintensities in Alzheimer disease, cerebral amyloid angiopathy, and healthy aging, Stroke 39 (4) (2008) 1127–1133.

[19] A.W. Bero, et al., Neuronal activity regulates the regional vulnerability to amyloid–beta deposition, Nat. Neurosci. 14 (6) (2011) 750–756.

[20] A.M. Brickman, Contemplating Alzheimer's disease and the contribution of white matter hyperintensities, Curr. Neurol. Neurosci. Rep. 13 (12) (2013) 415.

[21] A. Kapasi, C. DeCarli, J.A. Schneider, Impact of multiple pathologies on the threshold for clinically overt dementia, Acta Neuropathol. 134 (2) (2017) 171–186.

[22] B. Yew, D.A. Nation, I. Alzheimer's, Disease Neuroimaging, Cerebrovascular resistance: effects on cognitive decline, cortical atrophy, and progression to dementia, Brain 140 (7) (2017) 1987–2001.

[23] K.J. Bangen, et al., Cerebral blood flow and amyloid-beta interact to affect memory performance in cognitively normal older adults, Front. Aging Neurosci. 9 (2017) 181.

[24] A. Fazlollahi, et al., Increased cerebral blood flow with increased amyloid burden in the preclinical phase of alzheimer's disease, J. Magn. Reson. Imaging (2019).

[25] F.C. Maier, et al., Longitudinal PET-MRI reveals beta-amyloid deposition and rCBF dynamics and connects vascular amyloidosis to quantitative loss of perfusion, Nat. Med. 20 (12) (2014) 1485–1492.

[26] N. Mattsson, et al., Association of brain amyloid-beta with cerebral perfusion and structure in Alzheimer's disease and mild cognitive impairment, Brain 137 (Pt 5) (2014) 1550–1561.

[27] C.R. Jack Jr., et al., Tracking pathophysiological processes in Alzheimer's disease: an updated hypothetical model of dynamic biomarkers, Lancet Neurol. 12 (2) (2013) 207–216.

[28] J. Sepulcre, et al., In vivo tau, amyloid, and gray matter profiles in the aging brain, J. Neurosci. 36 (28) (2016) 7364–7374.

[29] D.R. Thal, J. Attems, M. Ewers, Spreading of amyloid, tau, and microvascular pathology in Alzheimer's disease: findings from neuropathological and neuroimaging studies, J Alzheimers Dis 42 (Suppl 4) (2014) S421–S429.

[30] A.G. Vlassenko, et al., Spatial correlation between brain aerobic glycolysis and amyloid-beta (Abeta) deposition, Proc. Natl. Acad. Sci. USA 107 (41) (2010) 17763–17767.

[31] O.B. Paulson, et al., Cerebral blood flow response to functional activation, J. Cereb. Blood Flow Metab. 30 (1) (2010) 2–14.

[32] L. Welberg, Brain metabolism: astrocytes bridge the gap, Nat. Rev. Neurosci. 10 (2) (2009) 86-86.

[33] M.J. Grothe, et al., Molecular properties underlying regional vulnerability to Alzheimer's disease pathology, Brain 141 (9) (2018) 2755–2771.

[34] B. Winblad, K. Palmer, M. Kivipelto, et al., Mild cognitive impairment–beyond controversies, towards a consensus: report of the International Working Group on Mild Cognitive Impairment., J. Intern. Med. (2004).